

两个二苯醚四羧酸-钴(II)配位聚合物的合成、结构和催化性质

赵素琴^{*,1} 顾金忠^{*,2}

(¹青海民族大学物理与电子信息工程学院, 西宁 810007)

(²兰州大学化学化工学院, 兰州 730000)

摘要: 采用水热方法, 选用2,3,3',4'-二苯醚四羧酸(H₄deta)和2,2'-联咪唑(H₂biim)、菲咯啉(phen)分别与CoCl₂·6H₂O在160 °C下反应, 得到了一维链结构([Co₂(μ₃-deta)(H₂biim)₃(H₂O)₂]_n, **1**)和二维网络结构([Co₂(μ₆-deta)(phen)₂·H₂O]_n, **2**)的配位聚合物, 并对其结构和催化性质进行了研究。研究表明, 在室温下配合物**1**在Knoevenagel缩合反应中显示出很好的催化活性。

关键词: 配位聚合物; 四羧酸; 催化性质; Knoevenagel缩合反应

中图分类号: O614.81*2 文献标识码: A 文章编号: 1001-4861(2022)01-0161-10

DOI: 10.11862/CJIC.2022.004

Synthesis, Structures and Catalytic Activity in Knoevenagel Condensation Reaction of Two Diphenyl Ether Tetracarboxylic Acid-Co(II) Coordination Polymers

ZHAO Su-Qin^{*,1} GU Jin-Zhong^{*,2}

(¹College of Physics and Electronic Information Engineering, Qinghai University for Nationalities, Xining 810007, China)

(²College of Chemistry and Chemical Engineering, Lanzhou University, Lanzhou 730000, China)

Abstract: Two cobalt(II) coordination polymers, namely [Co₂(μ₃-deta)(H₂biim)₃(H₂O)₂]_n (**1**) and {[Co₂((μ₆-deta)(phen)₂·H₂O)]_n (**2**), have been constructed hydrothermally using H₄deta (2,3,3',4'-diphenyl ether tetracarboxylic acid), H₂biim (2,2'-biimidazole), phen (1,10-phenanthroline), and cobalt chloride at 160 °C. The products were isolated as stable crystalline solids and were characterized by IR spectra, elemental analyses, thermogravimetric analyses, and single-crystal X-ray diffraction analyses. Single-crystal X-ray diffraction analyses revealed that compounds **1** and **2** crystallize in the triclinic and monoclinic systems, space groups $P\bar{1}$ and $P2_1/c$, respectively. Compound **1** discloses a 1D chain structure, and compound **2** features a 2D network. The catalytic activities in Knoevenagel condensation reaction of the compounds were investigated. Compound **1** exhibited excellent catalytic activity in Knoevenagel condensation reaction at room temperature. CCDC: 2069400, **1**; 2069401, **2**.

Keywords: coordination polymer; tetracarboxylic acid; catalytic property; Knoevenagel condensation reaction

0 Introduction

The field of coordination polymers has attracted tremendous attention due to their structural and topological diversity as well as their potential applications as functional materials^[1-11]. In the last ten years, organic

carboxylate ligands have been widely used in synthesizing coordination polymers due to the strong coordination ability of the carboxyl group and the rich coordination modes^[5-6,12-15]. Among them, ether-bridged carboxylic acids have been extensively applied as versatile building blocks toward the assembly of metal-organic

收稿日期: 2021-07-28。收修改稿日期: 2021-09-25。

青海省应用基础研究项目(No.2020-ZJ-705)资助。

*通信联系人。E-mail: qzhhsq@sina.com, gujzh@lzu.edu.cn

architectures^[16-17].

The 2,3,3',4'-diphenyl ether tetracarboxylic acid (H₄deta) is a good bridging ligand for constructing coordination polymers^[18], under considering structural semi-rigidity, which has multiple coordinate sites involving four carboxylate oxygen atoms and one O-ether donor. Knoevenagel condensation is one of the imperative and essential condensation processes in synthetic organic chemistry, in which α , β -unsaturated products formed via carbon-carbon double bond involve a nucleophilic addition reaction between active methylene and carbonyl compounds followed by a dehydration reaction^[19-23]. Products obtained are extensively used as specialty chemicals and intermediates in the synthesis of fine chemicals such as carbocyclic, substituted alkenes, biologically active compounds, therapeutic drugs, calcium antagonists, natural products, functional polymers, coumarin derivatives, flavors, and perfumes. Transition metal-catalyzed Knoevenagel condensation reactions have recently received much attention^[24-26], mainly due to the low price and moderate toxicity of the catalysts in combination with their high activity.

Herein, we report the synthesis, crystal structures, and catalytic activity of two Co(II) coordination polymers with H₄deta, 2,2'-biimidazole (H₂biim) and 1,10-phenanthroline (phen) ligands.

1 Experimental

1.1 Reagents and physical measurements

All chemicals and solvents were of AR grade and used without further purification. Carbon, hydrogen and nitrogen were determined using an Elementar Vario EL elemental analyzer. IR spectra were recorded using KBr pellets and a Bruker EQUINOX 55 spectrometer. Thermogravimetric analysis (TGA) data were collected on a LINSEIS STA PT1600 thermal analyzer with a heating rate of 10 °C · min⁻¹. Powder X-ray diffraction patterns (PXRD) were measured on a Rigaku-Dmax 2400 diffractometer using Cu K α radiation (λ = 0.154 06 nm); the X-ray tube was operated at 40 kV and 40 mA; the data collection range was between 5° and 45°. Solution ¹H NMR spectra were recorded on a JNM ECS 400M spectrometer.

1.2 Synthesis of [Co₂(μ_3 -deta)(H₂biim)₃(H₂O)₂]_n (1)

A mixture of CoCl₂ · 6H₂O (0.048 g, 0.2 mmol), H₄deta (0.035 g, 0.1 mmol), H₂biim (0.027 g, 0.2 mmol), NaOH (0.016 g, 0.4 mmol), and H₂O (10 mL) was stirred at room temperature for 15 min, and then sealed in a 25 mL Teflon-lined stainless-steel vessel, and heated at 120 °C for 3 d, followed by cooling to room temperature at a rate of 10 °C · h⁻¹. Orange block-shaped crystals were isolated manually, and washed with distilled water. Yield: 35% (based on H₄deta). Anal. Calcd. for C₃₄H₂₈Co₂N₁₂O₁₁(%): C 45.45, H 3.14, N 18.71; Found(%): C 45.62, H 3.12, N 18.59. IR (KBr, cm⁻¹): 3 384m, 2 972w, 1 628w, 1 549s, 1 483m, 1 430m, 1 398s, 1 377s, 1 341m, 1 271w, 1 231w, 1 182w, 1 120w, 1 084w, 1 049w, 991w, 907w, 867w, 828w, 756w, 694m, 624w.

1.3 Synthesis of {[Co₂(μ_6 -deta)(phen)₂] · H₂O}_n (2)

Synthesis of **2** was similar to **1** except using phen (0.040 g, 0.2 mmol) instead of H₂biim. Purple block-shaped crystals of **2** were isolated manually, and washed with distilled water. Yield: 60% (based on H₄deta). Anal. Calcd. for C₄₀H₂₄Co₂N₄O₁₀(%): C 57.30, H 2.88, N 6.68; Found(%): C 57.12, H 2.86, N 6.70. IR (KBr, cm⁻¹): 3 660w, 3 428w, 3 066w, 1 626s, 1 581s, 1 514m, 1 492w, 1 425m, 1 391s, 1 377s, 1 302w, 1 262w, 1 235w, 1 151w, 1 089w, 969w, 924w, 894w, 840m, 818w, 770m, 725m, 685w, 641w.

The compounds are insoluble in water and common organic solvents, such as methanol, ethanol, acetone, and DMF.

1.4 Structure determination

Two single crystals with dimensions of 0.25 mm × 0.20 mm × 0.18 mm (**1**) and 0.23 mm × 0.22 mm × 0.20 mm (**2**) were collected at 293(2) K on a Bruker SMART APEX II CCD diffractometer with Mo K α (λ = 0.071 073 nm). The structures were solved by direct methods and refined by full-matrix least-squares on F^2 using the SHELXTL-2014 program^[27]. All non-hydrogen atoms were refined anisotropically. All the hydrogen atoms were positioned geometrically and refined using a riding model. A summary of the crystallography data and structure refinements for **1** and **2** is given in Table 1. The selected bond lengths and angles for

compounds **1** and **2** are listed in Table 2. Hydrogen bond parameters of compounds **1** and **2** are given in Table 3 and 4. CCDC: 2069400, **1**; 2069401, **2**.

Table 1 Crystal data for compounds **1** and **2**

Parameter	1	2
Chemical formula	C ₃₄ H ₂₈ Co ₂ N ₁₂ O ₁₁	C ₄₀ H ₂₄ Co ₂ N ₄ O ₁₀
Molecular weight	898.54	838.49
Crystal system	Triclinic	Monoclinic
Space group	$P\bar{1}$	$P2_1/c$
<i>a</i> / nm	0.740 11(6)	1.107 14(10)
<i>b</i> / nm	1.022 55(14)	1.586 84(10)
<i>c</i> / nm	2.421 49(13)	1.997 32(15)
α / (°)	100.288(8)	
β / (°)	91.398(6)	105.398(9)
γ / (°)	100.304(9)	
<i>V</i> / nm ³	1.771(3)	3.383(5)
<i>Z</i>	2	4
<i>F</i> (000)	916	1 704
θ range for data collection / (°)	3.326-25.048	3.327-25.049
Limiting indices	$-8 \leq h \leq 8, -11 \leq k \leq 12, -28 \leq l \leq 21$	$-13 \leq h \leq 8, -18 \leq k \leq 18, -21 \leq l \leq 23$
Reflection collected, unique (<i>R</i> _{int})	6 257, 3 869 (0.062 9)	5 979, 3 420 (0.105 7)
<i>D</i> _c / (g·cm ⁻³)	1.685	1.646
μ / mm ⁻¹	1.019	1.052
Data, restraint, parameter	6 257, 1, 556	5 979, 1, 505
Goodness-of-fit on <i>F</i> ²	1.041	1.023
Final <i>R</i> indices [$I \geq 2\sigma(I)$] <i>R</i> ₁ , <i>wR</i> ₂	0.064 9, 0.129 2	0.059 5, 0.092 6
<i>R</i> indices (all data) <i>R</i> ₁ , <i>wR</i> ₂	0.113 2, 0.169 2	0.118 6, 0.117 4
Largest diff. peak and hole / (e·nm ⁻³)	583 and -846	577 and -537

Table 2 Selected bond distances (nm) and bond angles (°) for compounds **1** and **2**

1					
Co1—O1	0.218 4(4)	Co1—O4A	0.234 5(5)	Co1—N1	0.214 9(4)
Co1—N4	0.207 5(4)	Co1—N5	0.215 9(4)	Co1—N8	0.210 2(4)
Co2—O6	0.214 7(4)	Co2—O7	0.219 7(4)	Co2—O10	0.201 9(4)
Co2—O11	0.218 0(4)	Co2—N9	0.208 2(5)	Co2—N12	0.218 1(5)
N4—Co1—N8	178.6(2)	N1—Co1—N4	79.30(16)	N8—Co1—N1	101.12(16)
N4—Co1—N5	100.74(17)	N5—Co1—N8	78.77(17)	N1—Co1—N5	177.4(2)
O1—Co1—N4	94.65(17)	N8—Co1—O1	86.67(17)	N1—Co1—O1	90.06(17)
N5—Co1—O1	92.56(17)	N4—Co1—O4A	87.12(17)	N8—Co1—O4A	91.55(17)
N1—Co1—O4A	89.88(17)	N5—Co1—O4A	87.50(17)	O1—Co1—O4A	178.18(14)
O10—Co2—N9	104.93(19)	O10—Co2—O6	154.36(18)	O6—Co2—N9	100.53(17)
O11—Co2—O10	87.77(15)	O11—Co2—N9	88.52(18)	O11—Co2—O6	89.95(15)
O10—Co2—N12	98.07(16)	N9—Co2—N12	79.5(2)	O6—Co2—N12	89.37(16)
O11—Co2—N12	167.7(2)	O10—Co2—O7	93.96(16)	O7—Co2—N9	160.77(16)
O6—Co2—O7	60.89(15)	O11—Co2—O7	95.92(17)	O7—Co2—N12	94.47(18)

Continued Table 2

2					
Co1—O1	0.209 0(4)	Co1—O4A	0.209 0(3)	Co1—O7B	0.209 4(4)
Co1—O8B	0.210 6(3)	Co1—N1	0.213 3(4)	Co1—N2	0.215 8(4)
Co2—O2	0.202 4(3)	Co2—O3A	0.202 7(3)	Co2—O8B	0.206 3(4)
Co2—O9B	0.239 0(4)	Co2—N3	0.208 8(5)	Co2—N4	0.214 8(4)
O1—Co1—O4A	90.88(15)	O4A—Co1—O7B	100.25(14)	O1—Co1—O7B	166.12(14)
O8B—Co1—O4A	88.86(13)	O1—Co1—O8B	90.97(13)	O7B—Co1—O8B	81.08(13)
O4A—Co1—N1	90.22(16)	O1—Co1—N1	105.00(15)	O7B—Co1—N1	83.39(16)
O8B—Co1—N1	164.02(15)	O4A—Co1—N2	164.18(15)	O1—Co1—N2	83.49(16)
O7B—Co1—N2	87.76(15)	O8B—Co1—N2	105.96(14)	N1—Co1—N2	77.07(16)
O2—Co2—O3A	96.20(14)	O2—Co2—O8B	90.71(14)	O8B—Co2—O3A	100.16(15)
O2—Co2—N3	95.43(16)	N3—Co2—O3A	100.80(16)	N3—Co2—O8B	157.36(15)
N4—Co2—O2	170.27(15)	N4—Co2—O3A	92.39(15)	N4—Co2—O8B	92.28(16)
N3—Co2—N4	78.41(18)	O2—Co2—O9B	89.72(13)	O3A—Co2—O9B	158.05(15)
O9B—Co2—O8B	58.52(12)	N3—Co2—O9B	99.65(15)	N4—Co2—O9B	83.96(14)

Symmetry codes: A: $x, y-1, z$ for **1**; A: $-x+1, y+1/2, -z+1/2$; B: $x+1, y, z$ for **2**.

Table 3 Hydrogen bond parameters of compound 1

D—H...A	$d(\text{D—H}) / \text{nm}$	$d(\text{H...A}) / \text{nm}$	$d(\text{D...A}) / \text{nm}$	$\angle \text{DHA} / (^\circ)$
N2—H1...O2A	0.094 7	0.178 4	0.272 3	170.51
N3—H2...O1A	0.081 9	0.199 5	0.279 1	163.95
N6—H3...O3B	0.091 4	0.177 7	0.268 1	169.88
N7—H5...O4B	0.087 3	0.188 8	0.275 0	169.01
N10—H11...O9C	0.072 5	0.204 4	0.271 4	154.08
N11—H12...O9C	0.085 1	0.191 5	0.274 3	163.89
O10—H1W...O8D	0.082 0	0.179 0	0.261 0	177.84
O10—H2W...O7E	0.085 0	0.190 6	0.275 6	179.75
O11—H3W...O8D	0.085 5	0.193 2	0.278 5	175.56

Symmetry codes: A: $x-1, y, z$; B: $x+1, y-1, z$; C: $x-1, y-1, z$; D: $-x+2, -y+1, -z+1$; E: $-x+1, -y+1, -z+1$.

Table 4 Hydrogen bond parameters of compound 2

D—H...A	$d(\text{D—H}) / \text{nm}$	$d(\text{H...A}) / \text{nm}$	$d(\text{D...A}) / \text{nm}$	$\angle \text{DHA} / (^\circ)$
O10—H1W...O6	0.086 3	0.206 1	0.280 7	144.38
O10—H2W...N2A	0.085 0	0.264 9	0.349 9	179.65

Symmetry code: A: $-x+1, y+1/2, -z+1/2$.

1.5 Catalytic activity for Knoevenagel condensation reaction of aldehydes

Prior to the catalytic activity study, compound **1** was activated in a vacuum oven at 210 °C for 10 h. In a typical test, a suspension of an aromatic aldehyde (0.50 mmol, benzaldehyde as a model substrate), malononitrile (1.0 mmol), and catalyst (Molar fraction: 2%) in methanol (1.0 mL) was stirred at room temperature. After the desired reaction time, the catalyst was

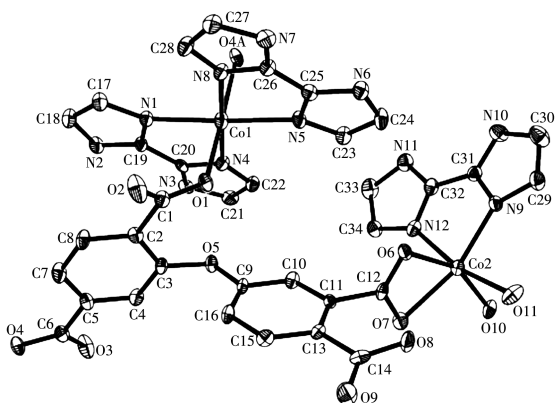
removed by centrifugation, followed by evaporation of the solvent from the filtrate under reduced pressure to give a crude solid. This solid was dissolved in CDCl_3 and analyzed by ^1H NMR spectroscopy for quantification of products (Fig. S1, Supporting information). To perform the recycling experiment, the catalyst was isolated by centrifugation, washed with dichloromethane, dried at room temperature, and reused. The subsequent steps were performed as described above.

2 Results and discussion

2.1 Description of the structure

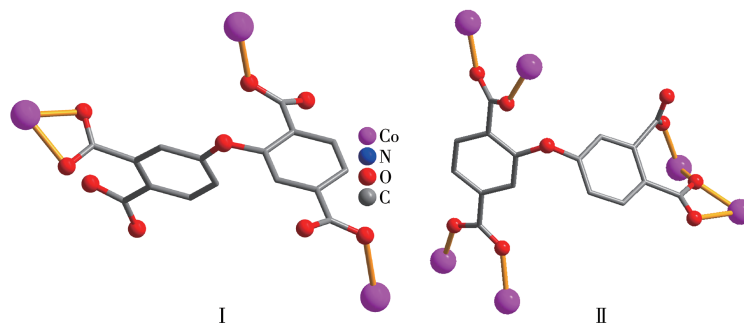
2.1.1 Structure of compound 1

X-ray crystallography analysis reveals that compound **1** crystallizes in the triclinic system space group $P\bar{1}$. As shown in Fig.1, the asymmetric unit of **1** bears two crystallographically unique Co(II) ions (Co1 and Co2), one μ_3 -deta⁴⁻ block, three H₂biim moieties, and two H₂O ligands. The six-coordinated Co1 ion exhibits a distorted octahedral {CoN₄O₂} environment, which is occupied by two carboxylate O donors from two different μ_3 -deta⁴⁻ blocks and four N atoms from two H₂biim moieties. The Co2 center is also six-coordinated and forms a distorted octahedral {CoN₂O₄} geometry. It is completed by two carboxylate O atoms from one μ_3 -deta⁴⁻ block, two O donors from two H₂O ligands, and two N atoms from the H₂biim moiety. The Co—O and Co—N bond distances are 0.218 4(4)-0.234 5(5) nm and 0.207 5(4)-0.218 1(5) nm, respectively; these are



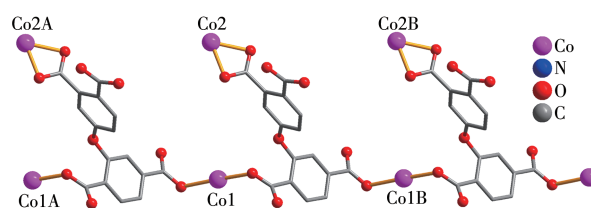
H atoms are omitted for clarity; Symmetry code: A: $x, y-1, z$

Fig.1 Drawing of asymmetric unit of compound **1** with 30% probability thermal ellipsoids



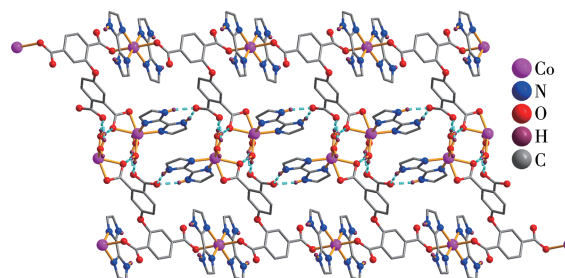
Scheme 1 Coordination modes of deta⁴⁻ ligand in compounds **1** and **2**

within the normal ranges observed in related Co(II) compounds^[6,28-29]. In compound **1**, the ligand deta⁴⁻ adopts a coordination mode I (Scheme 1) with four COO⁻ groups being uncoordinated, monodentate or bidentate. In deta⁴⁻ ligand, a dihedral angle (between two aromatic rings) and a C—O_{ether}—C angle are 78.88° and 118.26°, respectively. The μ_3 -deta⁴⁻ blocks connect Co ions to give a 1D chain (Fig.2). Adjacent chains are assembled into a 2D supramolecular sheet through O—H...O and N—H...O hydrogen bonds (Table 3 and Fig.3).



H₂biim and H₂O ligands are omitted for clarity; Symmetry codes: A: $x, y-1, z$; B: $x, y+1, z$

Fig.2 Perspective of 1D metal-organic chain along a axis



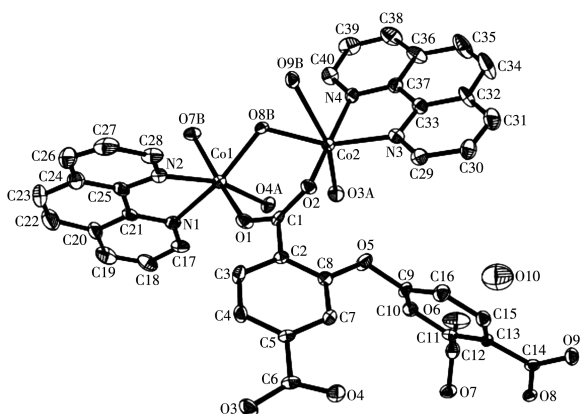
Dashed lines present the hydrogen bonds

Fig.3 Perspective of 2D H-bonded network along a axis

2.1.2 Structure of compound 2

The asymmetric unit of compound **2** contains two crystallographically unique Co(II) ions (Co1 and Co2), one μ_6 -deta⁴⁻ block, two phen moieties, and one lattice

water molecule. As depicted in Fig.4, both Co centers are six-coordinated and display a distorted octahedral $\{\text{CoN}_2\text{O}_4\}$ geometry. It is taken by four carboxylate O atoms from three individual μ_6 -deta⁴⁻ blocks and two N donors from the ligand phen. The bond lengths of Co—O are in a range of 0.202 4(3)-0.239 0(4) nm, while the Co—N bonds are 0.208 8(5) - 0.215 8(4) nm, being comparable to those found in some reported Co(II) compounds^[28-30]. In **2**, the deta⁴⁻ block acts as a μ_6 -linker (mode II, Scheme 1), in which four carboxylate groups adopt monodentate, μ -bridging bidentate or tridentate modes. Besides, the μ_6 -deta⁴⁻ ligand is considerably bent showing a dihedral angle of 67.68° (between two aromatic rings) and the angle of C—O_{ether}—C being 121.04°. Two adjacent Co1 and Co2 ions are joined via three carboxylate groups from three independent μ_6 -deta⁴⁻ ligands to form a Co₂ subunit with a Co1...Co2 distance of 0.352 7(2) nm (Fig.4). These di-cobalt(II) subunits are further linked together through the remaining carboxylate groups of μ_6 -deta⁴⁻ blocks to form a 2D metal-organic network (Fig. 5). Compounds **1** and **2** were assembled under similar conditions except for the type of auxiliary ligand used (H₂biim for **1** and phen for **2**), but they show different structures.

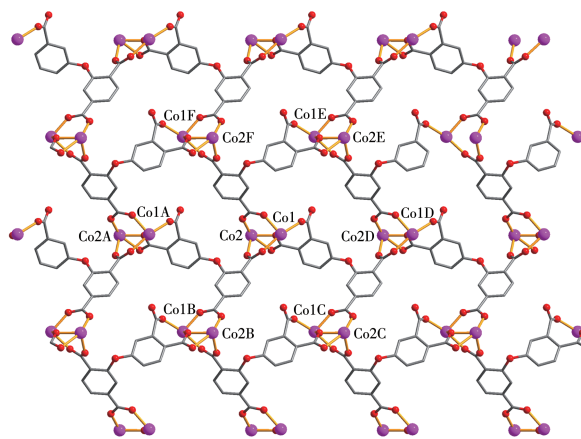


H atoms are omitted for clarity; Symmetry codes: A: $-x+1, y+1/2, -z+1/2$; B: $x+1, y, z$

Fig.4 Drawing of asymmetric unit of compound **2** with 30% probability thermal ellipsoids

2.2 TGA for compounds **1** and **2**

To determine the thermal stability of compounds **1** and **2**, their thermal behaviors were investigated under nitrogen atmosphere by TGA. As shown in Fig. 6,



Phen ligands are omitted for clarity; Symmetry codes: A: $x-1, y, z$; B: $-x+1, y-1/2, -z+1/2$; C: $-x+2, y-1/2, -z+1/2$; D: $x+1, y, z$; E: $-x+2, y+1/2, -z+1/2$; F: $-x+1, y+1/2, -z+1/2$

Fig.5 View of 2D metal-organic network parallel to *ab* plane

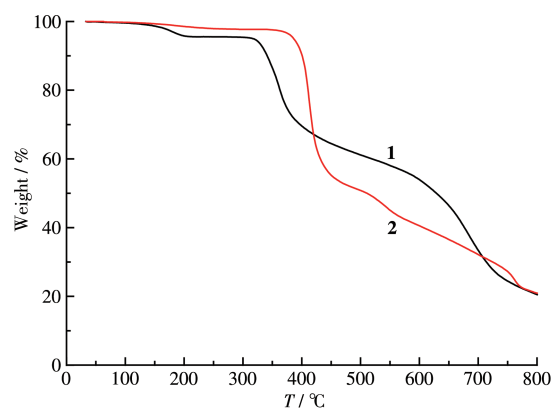


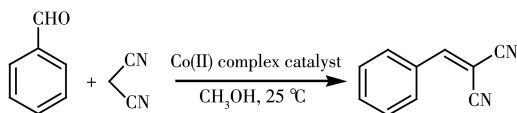
Fig.6 TGA curves of compounds **1** and **2**

compound **1** lost its two coordinated water molecules in a range of 96 - 203 °C (Obsd. 4.2%, Calcd. 4.0%). Decomposition of the sample occurred above 305 °C, corresponding to the removal of deta⁴⁻ and H₂biim ligands attached to the Co ions. For **2**, one weight loss (Obsd. 2.2%, Calcd. 2.1%) in a range of 84 - 243 °C corresponds to the removal of one lattice water molecule; the remaining sample started to decompose above 342 °C, corresponding to the removal of deta⁴⁻ and phen ligands attached to the Co ions.

2.3 Catalytic activity for Knoevenagel condensation reaction

Given the potential of cobalt(II) coordination compounds to catalyze organic reactions^[6,30-31], we explored the application of **1** and **2** as heterogeneous catalysts in the Knoevenagel condensation reaction of benzalde-

hyde as a model substrate to give 2-(phenylmethylene)-propanedinitrile. Typical tests were carried out by reacting a mixture of benzaldehyde, malononitrile, and a Co(II) complex catalyst in methanol at room temperature (Scheme 2, Table 5). Such effects as reaction time, catalyst loading, solvent composition, catalyst recycling, and finally substrate scope were investigated.



Scheme 2 Knoevenagel condensation reaction of benzaldehyde (model substrate) catalyzed by Co(II) coordination compounds

Upon using compound **1** as the catalyst (Molar fraction: 2%), a high conversion rate of 100% of benzaldehyde into 2-(phenylmethylene)-propanedinitrile was reached after 60 min in methanol at room temperature (Table 5, Entry 6). The product was accumulated with a yield increase from 41% to 100% on prolonging the reaction from 10 to 60 min (Table 5, Entry 1-6). The influence of catalyst amount was also investigated, revealing a product yield growth from 92% to 100% on

increasing the loading of catalyst from 1% to 2.5% (Table 5, Entry 6 and 11-13). In addition to water, other solvents were tested, in particular, the reaction showed a comparable efficiency in H₂O and ethanol (90% and 98% product yields, respectively). Acetonitrile and chloroform were less suitable (85% and 67% product yields, respectively). It should be highlighted that under similar reaction conditions, the Knoevenagel condensation of benzaldehyde was significantly less efficient in the absence of catalyst (only 23% product yield) or when using H₄deta (30% yield) or CoCl₂·6H₂O (33% yield) as catalysts (Table 5, Entry 15-17).

The results show that compound **1** is more active than compound **2**. Although a relationship between structure and catalytic activity in the present study can not be clearly established, the highest conversion shown by compound **1** may eventually be associated with its 1D structure for easily accessible metal centers, together with the presence of the open metal sites^[30,32].

We also compared the activities of catalyst **1** in the reactions of other substituted aromatic aldehydes with malononitrile, and the corresponding yields were in a range of 54% to 100% (Table 6). Aryl aldehydes

Table 5 Knoevenagel condensation reaction of benzaldehyde with malononitrile catalyzed by Co(II) coordination compounds

Entry	Catalyst	Time / min	Catalyst loading ^a / %	Solvent	Yield ^b / %
1	1	10	2.0	CH ₃ OH	41
2	1	20	2.0	CH ₃ OH	56
3	1	30	2.0	CH ₃ OH	64
4	1	40	2.0	CH ₃ OH	80
5	1	50	2.0	CH ₃ OH	93
6	1	60	2.0	CH ₃ OH	100
7	1	60	2.0	H ₂ O	90
8	1	60	2.0	C ₂ H ₅ OH	98
9	1	60	2.0	CH ₃ CN	85
10	1	60	2.0	CHCl ₃	67
11	1	60	1.0	CH ₃ OH	92
12	1	60	1.5	CH ₃ OH	98
13	1	55	2.5	CH ₃ OH	100
14	2	60	2.0	CH ₃ OH	89
15	Blank	60	—	CH ₃ OH	23
16	CoCl ₂ ·6H ₂ O	60	2.0	CH ₃ OH	33
17	H ₄ deta	60	2.0	CH ₃ OH	30

^a Molar fraction; ^b Calculated by ¹H NMR spectroscopy: $n_{\text{product}}/n_{\text{aldehyde}} \times 100\%$.

bearing strong electron-withdrawing substituents (*e.g.*, nitro and chloro) exhibited high activities (Table 6, Entry 2-5), which may be related to an increase in the electrophilicity of the substrate. Aldehydes containing electron-donating groups (*e.g.*, methyl) showed lower reaction yields (Table 6, Entry 6-8), as expected.

To examine the stability of **1** in the Knoevenagel condensation reaction, we tested the recyclability of this heterogeneous catalyst. For this purpose, upon completion of a reaction cycle, we separated the catalyst by centrifugation, washed it with CH₂Cl₂, and dried it at room temperature before its further use. We found

that for catalyst **1**, the catalytic system maintained the high activity over at least five consecutive cycles with the yields being 100%, 100%, 99%, and 98% for the second to the fifth run, respectively. According to the PXRD data (Fig.S2), the structure of **1** was essentially preserved after five catalytic cycles.

The achieved catalytic performance of compound **1** in the Knoevenagel condensation reaction of benzaldehyde with malononitrile is superior to those exhibited by the heterogeneous catalysts based on other metal-carboxylate coordination compounds (Table 7)^[33-37].

Table 6 Knoevenagel condensation reaction of various aldehydes with malononitrile catalyzed by compound **1**^a

Entry	Substituted benzaldehyde substrate (R—C ₆ H ₄ CHO)	Product yield ^b / %
1	R=H	100
2	R=2-NO ₂	100
3	R=3-NO ₂	100
4	R=4-NO ₂	100
5	R=4-Cl	100
6	R=4-OH	54
7	R=4-CH ₃	98
8	R=4-OCH ₃	76

^a Reaction conditions: aldehyde (0.5 mmol), malononitrile (1.0 mmol), catalyst **1** (Molar fraction: 2.0%), and CH₃OH (1.0 mL) at 25 °C; ^b Calculated by ¹H NMR spectroscopy: $n_{\text{product}}/n_{\text{aldehyde}} \times 100\%$.

Table 7 Comparison among various catalysts for Knoevenagel condensation reaction between benzaldehyde and malononitrile

Catalyst	Catalyst loading / %	Solvent	<i>t</i> / h	<i>T</i>	Product yield / %	Ref.
[Co ₂ (μ ₃ -deta)(H ₂ biim) ₃ (H ₂ O) ₂] _n	2	MeOH	1	RT	100	This work
Zn ₃ (OH)(ATTCA) ₂ (H ₂ O)]·C ₂ H ₆ NH ₂ ·4DMF·H ₂ O	10	CH ₂ Cl ₂	5	RT	94	[33]
[Zn ₃ (L) ₂ (μ ₂ -OH) ₂] _n	4	H ₂ O	8	90 °C	78	[34]
{[Ba ₃ Zn ₄ (TDP) ₂ (HCO ₂) ₂ (OH) ₂] ₂ ·7DMF·4H ₂ O} _n	3	Ethanol	1	60 °C	99	[35]
[Zn(L)(H ₂ O) ₂] _n · <i>n</i> (<i>N</i> -methylformamide)	3	MeOH	1.5	40 °C	75	[36]
[Pb(L) ₂] ₂ ·2DMF·6H ₂ O	3	CH ₃ CN	24	RT	100	[37]

3 Conclusions

In summary, we have synthesized two Co(II) coordination polymers based on a tetracarboxylate ligand. Compound **1** discloses a 1D chain structure. Compound **2** features a 2D network. The catalytic properties of both compounds were investigated. Compound **1** revealed an excellent catalytic activity in the Knoevenagel condensation reaction of benzaldehyde at room

temperature.

Supporting information is available at <http://www.wjhx.cn>

References:

- [1]Zheng X D, Lu T B. Constructions of Helical Coordination Compounds. *CrystEngComm*, **2010**,**12**(2):324-336
- [2]Fan W D, Yuan S, Wang W J, Feng L, Liu X P, Zhang X R, Wang X,

- Kang Z X, Dai F N, Yuan D Q, Sun D F, Zhou H C. Optimizing Multi-variate Metal-Organic Frameworks for Efficient C₂H₂/CO₂ Separation. *J. Am. Chem. Soc.*, **2020**,**142**(19):8728-8737
- [3]Wang H, Li J. Microporous Metal-Organic Frameworks for Adsorptive Separation of C5 - C6 Alkane Isomers. *Acc. Chem. Res.*, **2019**,**52**(7): 1968-1978
- [4]Xiao J D, Jiang H L. Metal-Organic Frameworks for Photocatalysis and Photothermal Catalysis. *Acc. Chem. Res.*, **2019**,**52**(2):356-366
- [5]Gu J Z, Wen M, Cai Y, Shi Z F, Arol A S, Kirillova M V, Kirillov A M. Metal-Organic Architectures Assembled from Multifunctional Polycarboxylates: Hydrothermal Self-Assembly, Structures, and Catalytic Activity in Alkane Oxidation. *Inorg. Chem.*, **2019**,**58**(4):2403-2412
- [6]Gu J Z, Wen M, Cai Y, Shi Z F, Nesterov D S, Kirillova M V, Kirillov A M. Cobalt(II) Coordination Polymers Assembled from Unexplored Pyridine-Carboxylic Acids: Structural Diversity and Catalytic Oxidation of Alcohols. *Inorg. Chem.*, **2019**,**58**(9):5875-5885
- [7]Roy M, Adhikary A, Mondal A K, Mondal R. Multifunctional Properties a 1D Helical Co(II) Coordination Polymers: Toward Single-Ion Magnetic Behavior and Efficient Dye Degradation. *ACS Omega*, **2018**, **3**(11):15315-15324
- [8]Salitros I, Herchel R, Fuhr O, Gonzalez-Prieto R, Ruben M. Polynuclear Iron(II) Complexes with 2,6-Bis(pyrazol-1-yl)-pyridineanthracene Ligands Exhibiting Highly Distorted High-Spin Centers. *Inorg. Chem.*, **2019**,**58**(7):4310-4319
- [9]Lustig W P, Mukherjee S, Rudd N D, Desai A V, Li J, Ghosh S K. Metal-Organic Frameworks: Functional Luminescent and Photonic Materials for Sensing Applications. *Chem. Soc. Rev.*, **2017**, **46**(10): 3242-3285
- [10]Cui Y J, Yue Y F, Qian G D, Chen B L. Luminescent Functional Metal-Organic Frameworks. *Chem. Rev.*, **2012**,**112**(2):1126-1162
- [11]Haddad S, Lúzaró I A, Fantham M, Mishra A, Silvestre-Albero J, Osterrieth J W M, Schierle G S K, Kaminski C F, Forgan R S, Fairen-Jimenez D. Design of a Functionalized Metal-Organic Framework System of Enhanced Targeted Delivery to Mitochondria. *J. Am. Chem. Soc.*, **2020**,**142**(14):6661-6674
- [12]Gu J Z, Wen M, Liang X X, Shi Z F, Kirillova M V, Kirillov A M. Multifunctional Aromatic Carboxylic Acids as Versatile Building Blocks for Hydrothermal Design of Coordination Polymers. *Crystals*, **2018**,**8**:83
- [13]赵素琴,顾金忠.基于原位配体反应的锰(II)配位聚合物的合成、结构和催化性质.无机化学学报,**2021**,**37**(4):751-757
ZHAO S Q, GU J Z. Synthesis, Structure and Catalytic Properties of Mn(II) Coordination Polymer through *In Situ* Ligand Reaction. *Chinese J. Inorg. Chem.*, **2021**,**37**(4):751-757
- [14]Li Y, Wu J, Gu J Z, Qiu W D, Feng A S. Temperature-Dependent Syntheses of Two Manganese(II) Coordination Compounds Based on an Ether-Bridged Tetracarboxylic Acid. *Chin. J. Struct. Chem.*, **2020**, **39**(4):727-736
- [15]Agarwal R A, Gupta A K, De D. Flexible Zn-MOF Exhibiting Selective CO₂ Adsorption and Efficient Lewis Acidic Catalytic Activity. *Cryst. Growth Des.*, **2019**,**19**(3):2010-2018
- [16]Gu J Z, Cai Y, Wen M, Shi Z F, Kirillov A M. A New Series of Cd(II) Metal-Organic Architectures Driven by Soft Ether-Bridged Tricarboxylate Spacers: Synthesis, Structural and Topological Versatility, and Photocatalytic Properties. *Dalton Trans.*, **2018**,**47**(40):14327-14339
- [17]Gu J Z, Liang X X, Cui Y H, Wu J, Shi Z F, Kirillov A M. Introducing 2-(2-Carboxyphenoxy)terephthalic Acid as a New Versatile Building Block for Design of Diverse Coordination Polymers: Synthesis, Structural Features, Luminescence Sensing, and Magnetism. *CrystEngComm*, **2017**,**19**(18):2570-2588
- [18]Li Y, Chen Y X, Zhao Z Y, Zou X Z, Feng A S. Syntheses, Crystal Structures, Luminescent and Magnetic Properties of Three Ni(II), Zn(II) and Cd(II) Coordination Polymers Based on an Ether-Bridged Tetracarboxylic Acid. *Chin. J. Struct. Chem.*, **2020**,**39**(4):967-977
- [19]Li G, Xiao J, Zhang W. Efficient and Reusable Amine-Functionalized Polyacrylonitrile Fiber Catalysts for Knoevenagel Condensation in Water. *Green Chem.*, **2012**,**14**:2234-2242
- [20]Elhamifar D, Kazempoor S, Karimi B. Amine-Functionalized Ionic Liquid-Based Mesoporous Organosilica as a Highly Efficient Nanocatalyst for the Knoevenagel Condensation. *Catal. Sci. Technol.*, **2016**,**6**:4318-4326
- [21]Dumbre D K, Mozammel T, Selvakannan P R, Hamid S B A, Choudhary V R, Bharagava S K. Thermally Decomposed Mesoporous Nickel Iron Hydroxalate: An Active Solid-Base Catalyst for Solvent-Free Knoevenagel Condensation. *J. Colloid Interface Sci.*, **2015**,**441**: 52-58
- [22]Wach A, Drozdek M, Dudek B, Szneler E, Kuśtrowski P. Control of Amine Functionality Distribution in Polyvinylamine/SBA-15 Hybrid Catalysts for Knoevenagel Condensation. *Catal. Commun.*, **2015**,**64**: 52-57
- [23]Xue L P, Li Z H, Zhang T, Cui J J, Gao Y, Yao J X. Construction of Two Zn(II)/Cd(II) Multifunctional Coordination Polymers with Mixed Ligands for Catalytic and Sensing Properties. *New J. Chem.*, **2018**,**42**: 14203-14209
- [24]Zhai Z W, Yang S H, Lv Y R, Du C X, Li L K, Zang S Q. Amino Functionalized Zn/Cd-Metal-Organic Frameworks for Selective CO₂ Adsorption and Knoevenagel Condensation Reactions. *Dalton Trans.*, **2019**,**48**(12):4007-4014
- [25]Yao C, Zhou S L, Kang X J, Zhao Y, Yan R, Zhang Y, Wen L L. A Cationic Zinc-Organic Framework with Lewis Acidic and Basic Bifunctional Sites as an Efficient Solvent-Free Catalyst: CO₂ Fixation and Knoevenagel Condensation Reaction. *Inorg. Chem.*, **2018**,**57** (17):11157-11164
- [26]Miao Z C, Luan Y, Qi C, Ramella D. The Synthesis of a Bifunctional Copper Metal Organic Framework and Its Application in the Aerobic Oxidation/Knoevenagel Condensation Sequential Reaction. *Dalton Trans.*, **2016**,**45**(35):13917-13924
- [27]Sheldrick G M. *SHELXL 97, Program for Refinement of Crystal Structure*. University of Göttingen, Germany, **1997**.
- [28]Gu J Z, Gao Z Q, Tang Y. pH and Auxiliary Ligand Influence on the Structural Variations of 5(2'-Carboxylphenyl) Nicotinate Coordination

- Polymers. *Cryst. Growth Des.*, **2012**, **12**(6):3312-3323
- [29] 顾文君, 顾金忠. 由半刚性三羧酸配体构筑的一维和二维钴(II)配位聚合物的合成、晶体结构及磁性质. *无机化学学报*, **2017**, **33**(2): 227-236
- GU W J, GU J Z. Syntheses, Crystal Structures and Magnetic Properties of 1D and 2D Cobalt(II) Coordination Polymers Constructed from Semi-rigid Tricarboxylic Acid. *Chinese J. Inorg. Chem.*, **2017**, **33**(2): 227-236
- [30] Laha B, Khullar S, Gogia A, Mandal S K. Effecting Structural Diversity in a Series of Co(II) - Organic Frameworks by the Interplay between Rigidity of a Dicarboxylate and Flexibility of Bis(tridentate) Spanning Ligands. *Dalton Trans.*, **2020**, **49**(35):12298-12310
- [31] Chand S, Pal S C, Mondal M, Hota S, Pal A, Sahoo R, Das M C. Three-Dimensional Co(II)-Metal-Organic Frameworks with Varying Porosities and Open Metal Sites toward Multipurpose Heterogeneous Catalysis under Mild Conditions. *Cryst. Growth Des.*, **2019**, **19**(9): 5343-5353
- [32] Loukopoulos E, Kostakis G E. Review: Recent Advances of One-Dimensional Coordination Polymers as Catalysts. *J. Coord. Chem.*, **2018**, **71**:371-410
- [33] Fan W, Wang Y, Xiao Z, Zhang L, Gong Y, Dai F, Wang R, Sun D. A Stable Amino-Functionalized Interpenetrated Metal-Organic Framework Exhibiting Gas Selectivity and Pore - Size - Dependent Catalytic Performance. *Inorg. Chem.*, **2017**, **56**(22):13634-13637
- [34] Wang X F, Zhou S B, Du C C, Wang D Z, Jia D. Seven New Zn(II)/Cd(II) Coordination Polymers with 2-(Hydroxymethyl)-1H-benzo[d]imidazole-5-carboxylic Acid: Synthesis, Structures and Properties. *J. Solid State Chem.*, **2017**, **252**:72-85
- [35] Chen H, Fan L, Hu T, Zhang X. 6s-3d {Ba₃Zn₄}-Organic Framework as an Effective Heterogeneous Catalyst for Chemical Fixation of CO₂ and Knoevenagel Condensation Reaction. *Inorg. Chem.*, **2021**, **60**(5): 3384-3392
- [36] Karmakar A, Rubio G M D M, Guedes da Silva M F C, Hazra S, Pombeiro A J L. Solvent-Dependent Structural Variation of Zinc(II) Coordination Polymers and Their Catalytic Activity in the Knoevenagel Condensation Reaction. *Cryst. Growth Des.*, **2015**, **15**(9): 4185 - 4197
- [37] Lin X M, Li T, Chen L F, Zhang L, Su C Y. Two Ligand-Functionalized Pb(II) Metal - Organic Frameworks: Structures and Catalytic Performances. *Dalton Trans.*, **2012**, **41**(34):10422-10429